

Supporting Information

Nucleoside-regulated catalytic activity of copper nanoclusters and its application for mercury ions detection

Shiyan Li,^{‡a} Zihang Zeng,^{‡a} Congcong Zhao,^a Haoyu Wang,^a Xiaosheng Ye^{b,c} and

*Taiping Qing^{*ac}*

^a College of Environment and Resources, Xiangtan University, Xiangtan 411105, Hunan Province, China

^b Xiangya School of Public Health, Central South University, Changsha 410078, Hunan, China.

^cState Key Laboratory of Chemo/Biosensing and Chemometrics, Hunan University, Changsha 410082, China

[‡]These authors contributed equally to this work.

^{*} To whom correspondence should be addressed. E-mail: taiping_qing@163.com

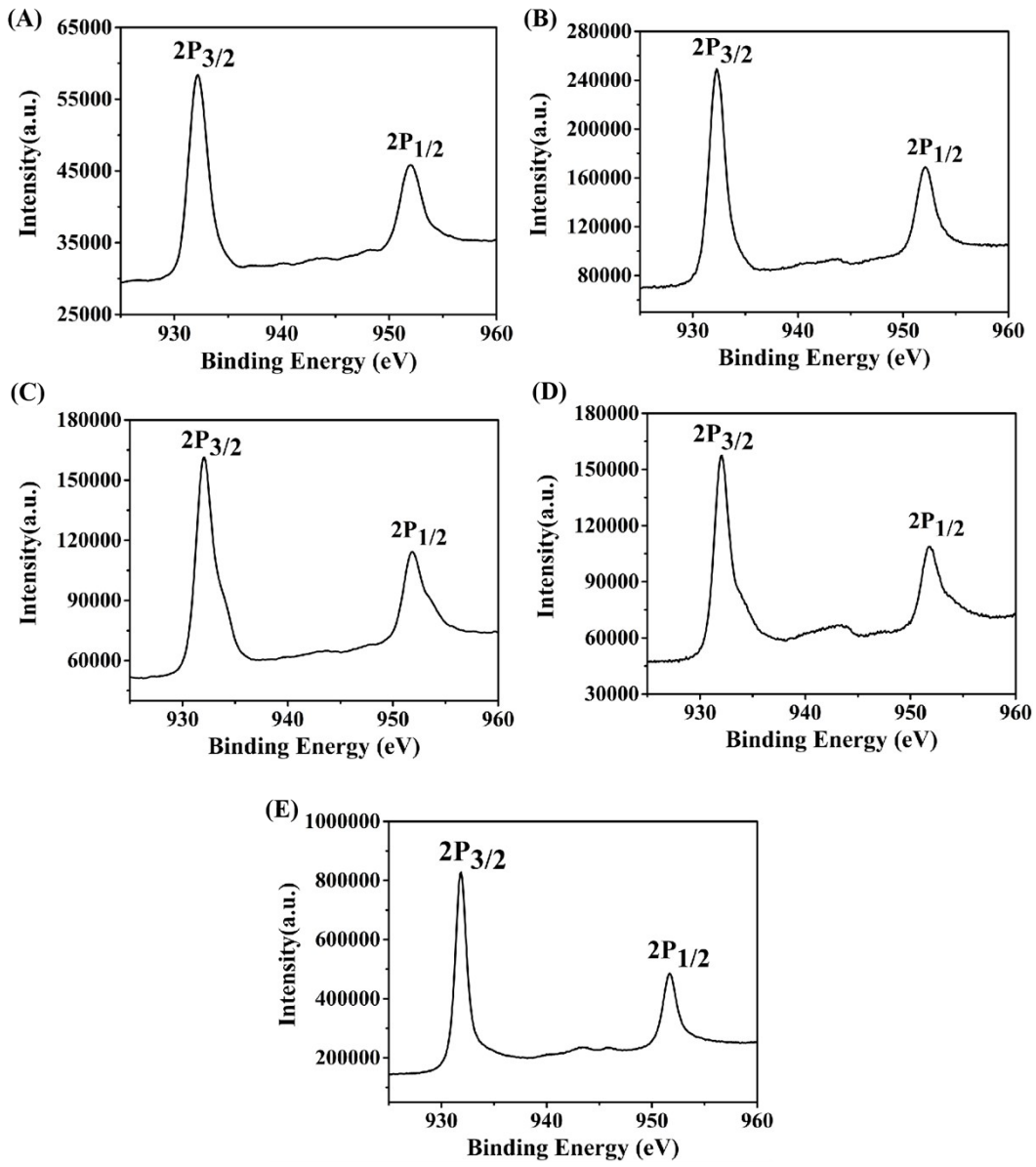


Fig. S1. XPS spectra obtained from different copper nanocluster (A-H: A-CuNCs, G-CuNCs, C-CuNCs, T-CuNCs, template free CuNCs), showing the $2\text{p}_{3/2}$ and Cu $2\text{p}_{1/2}$ peaks at 932.6 and 952.5 eV respectively indicating the presence of Cu(0)/Cu(I) state.

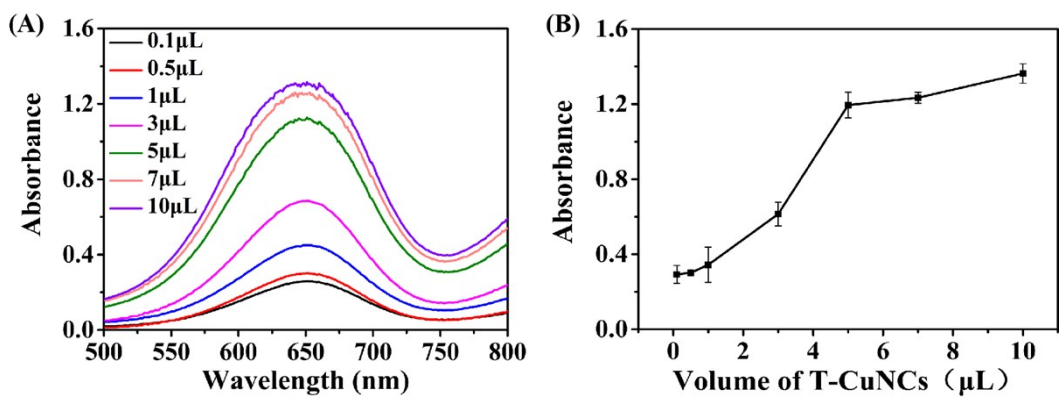


Fig. S2. Effect of T-CuNCs volume on the catalytic activity of T-CuNCs; (A) The effect of T-CuNCs volume on ultraviolet absorption spectrum of the catalytic system; (B) The effect of the T-CuNCs volume on the absorbance value of the system at 652nm.

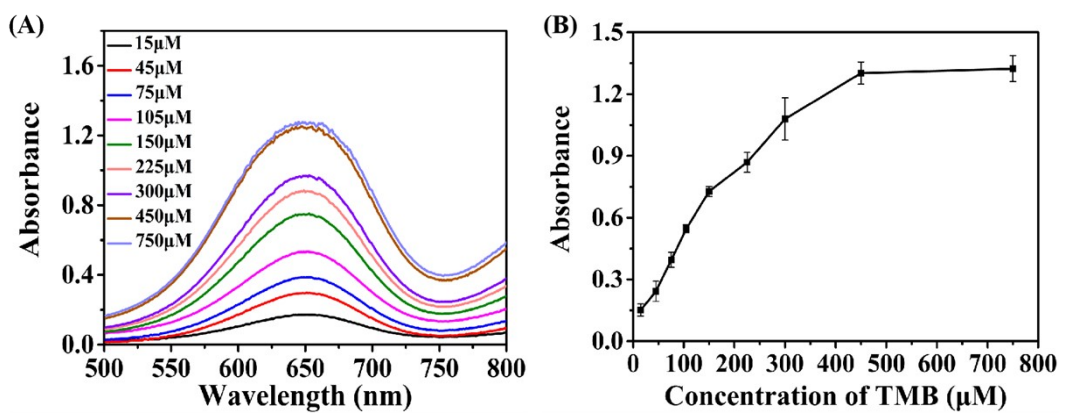


Fig. S3. Effect of TMB concentration on the catalytic activity of T-CuNCs; (A) The effect of TMB concentration on ultraviolet absorption spectrum of the catalytic system; (B) The effect of the TMB concentration on the absorbance value of the system at 652nm.

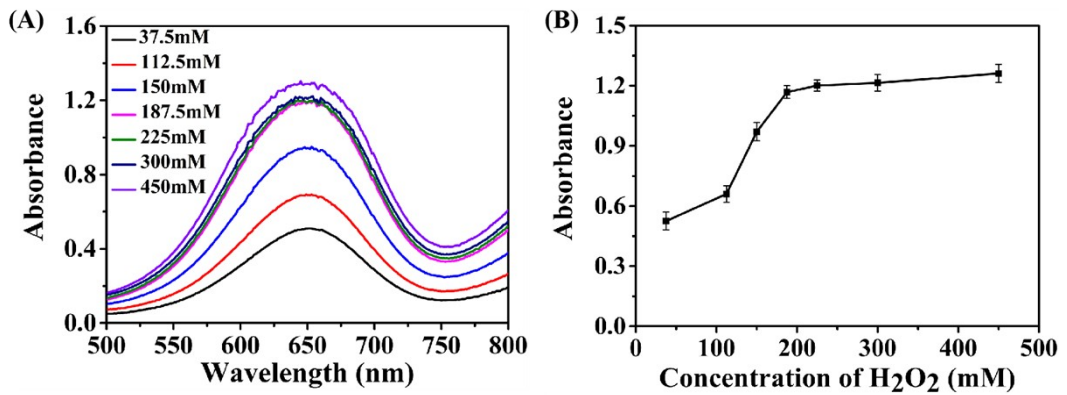


Fig. S4. Effect of H_2O_2 concentration on the catalytic activity of T-CuNCs; (A) The effect of H_2O_2 concentration on ultraviolet absorption spectrum of the catalytic system; (B) The effect of the H_2O_2 concentration on the absorbance value of the system at 652nm.

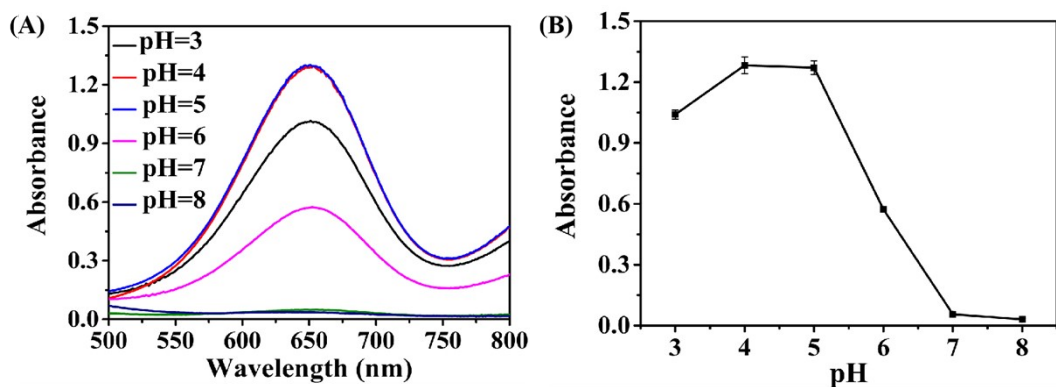


Fig. S5. Effect of pH on the catalytic activity of T-CuNCs; (A) The effect of pH on ultraviolet absorption spectrum of the catalytic system; (B) The effect of the pH on the absorbance value of the system at 652nm.

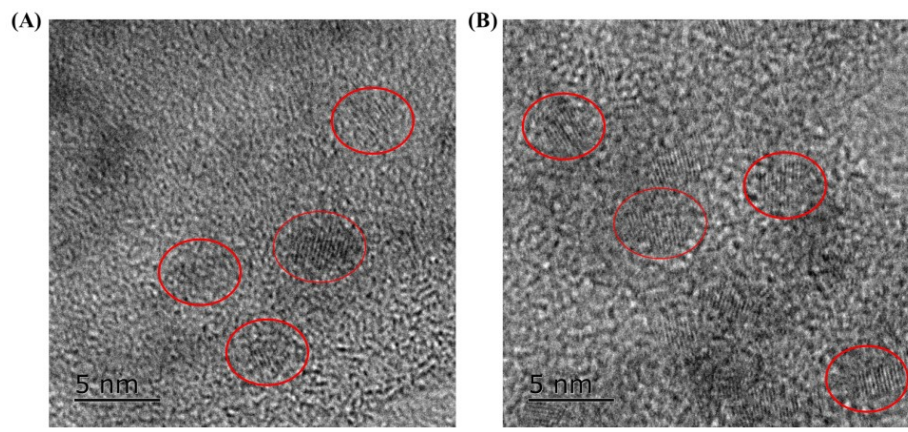


Fig. S6. TEM images of the effect of mercury ions on copper nanoclusters, (A) TEM of T-CuNCs; (B) TEM of T-CuNCs after added Hg^{2+} .

Table S1. Performance comparison of this work with other nanomaterials-based sensors for the detection of Hg^{2+} .

Materials	Linear range	LOD	Ref.
AuNPs	25–750 nM	50 nM	1
AgNPs	10–100 μM	2.2 μM	2
TPDT-AgNPs	/	5 μM	3
TPDT-gold nanorods	1–7 μM	0.317 μM	4
DNA-AuNPs	0–5 μM	0.5 μM	5
MoS_2 nanosheets	2–200 μM	0.5 μM	6
$\text{SiO}_2/\text{AgNPs}$	0–40 μM	5 μM	7
Cu@AuNPs	10–500 nM, 500–2500 nM	10 nM	8
MT-CuNCs	97 nM–2.325 μM , 3.10 μM –15.59 μM	43.8 nM	9
DNA-silica nanoparticles	0–500 nM	20 nM	10
CuNCs	0–350 μM	11.67 μM	This work

Reference

1. G.H. Chen, W.Y. Chen, Y.C. Yen, C.W. Wang, H.T. Chang, C.F. Chen, *Anal. Chem.*, 2014, **86**, 6843-6849.
2. K. Farhadia, M. Forougha, R. Molaeia, S. Hajizadeha, A. Rafipourb, *Sens. Actuators B Chem.*, 2012, **161**, 880-885.
3. P. Rameshkumar, P. Viswanathan, R. Ramaraj, *Sens. Actuators B Chem.*, 2014, **202**, 1070-1077,
4. S. Jayabal, R. Sathiyamurthi, R. Ramaraj, *J. Mater. Chem. A*, 2014, **2**, 8918-8925.
5. X. Xu, J. Wang, K. Jiao, X. Yang, *Biosens. Bioelectron.*, 2009, **10**, 3153-3158.
6. Y. Lu, J. Yu, W.C. Ye, Y. Xin, P.P. Zhou, H.X. Zhang, *Microchim. Acta*, 2016, **183**, 2481-2489.
7. P. Rameshkumar ,S. Manivannan ,R. Ramaraj, *J. Nanopart. Res.*, 2013, **15**, 1639-1647.
8. Y. Zhao, H. Qiang, Z.B. Chen, *Microchim. Acta*, 2017, **184**, 107-115.
9. R. Liu, L. Zuo, X. Huang, S. Liu, G. Yang, S. Li, C. Lv, *Microchim. Acta*, 2019, **186**, 250.
10. Y.F. Zhang, Q. Yuan, T. Chen, X.B. Zhang, Y. Chen, W.H. Tan, *Anal. Chem.*, 2012, **84**, 1956-1962.